റ്റ

Research article

Christian Heide*, Tobias Boolakee, Timo Eckstein and Peter Hommelhoff

Optical current generation in graphene: CEP control vs. $\omega + 2\omega$ control

https://doi.org/10.1515/nanoph-2021-0236 Received May 13, 2021; accepted July 2, 2021; published online July 21, 2021

Abstract: The injection of directional currents in solids with strong optical fields has attracted tremendous attention as a route to realize ultrafast electronics based on the quantum-mechanical nature of electrons at femto- to attosecond timescales. Such currents are usually the result of an asymmetric population distribution imprinted by the temporal symmetry of the driving field. Here we compare two experimental schemes that allow control over the amplitude and direction of light-field-driven currents excited in graphene. Both schemes rely on shaping the incident laser field with one parameter only: either the carrier-envelope phase (CEP) of a single laser pulse or the relative phase between pulses oscillating at angular frequencies ω and 2ω , both for comparable laser parameters. We observe that the efficiency in generating a current via two-color-control exceeds that of CEP control by more than two orders of magnitude (7 nA vs. 18 pA), as the $\omega + 2\omega$ field exhibits significantly more asymmetry in its temporal shape. We support this finding with numerical simulations that clearly show that two-color current control in graphene is superior, even down to single-cycle pulse durations. We expect our results to be relevant to

Christian Heide, Tobias Boolakee and Timo Eckstein contributed equally to this work.

*Corresponding author: Christian Heide, Department of Physics, Friedrich-Alexander-Universität Erlangen-Nürnberg (FAU), Staudtstrasse 1, Erlangen D-91058, Germany; and Stanford PULSE Institute, SLAC National Accelerator Laboratory, Menlo Park, California 94025, USA, E-mail: cheide@stanford.edu. https://orcid.org/0000-0002-7652-3241

Tobias Boolakee, Timo Eckstein and Peter Hommelhoff, Department of Physics, Friedrich-Alexander-Universität Erlangen-Nürnberg (FAU), Staudtstrasse 1, Erlangen D-91058, Germany,

E-mail: tobias.boolakee@fau.de (T. Boolakee),

Timo.Eckstein@fau.de (T. Eckstein),

peter.hommelhoff@physik.uni-erlangen.de (P. Hommelhoff).

https://orcid.org/0000-0001-7392-0893 (T. Boolakee). https:// orcid.org/0000-0002-6819-1865 (T. Eckstein). https://orcid.org/ 0000-0003-4757-5410 (P. Hommelhoff)

experimentally access fundamental properties of any solid at ultrafast timescales, as well as for the emerging field of petahertz electronics.

Keywords: carrier-envelope phase; current generation; graphene; two-color; ultrafast.

Dedicated to Professor Mark Stockman, with whom we intensely and with utmost pleasure and joy discussed strong-field physics in solids for many years - the last time when he spent a week with us in Erlangen in December 2019.

Controlling currents in solids using light fields is pivotal for ultrafast optoelectronics [1-8]. Furthermore, this ultrafast optical control might give direct access to novel solid-state properties, such as quantum-mechanical phases [5, 9-12], topological properties [13-20], ultrafast magnetism [21], and spin control [22], which are impossible to control with today's conventional electronics. Starting almost 30 years ago, early experiments used two optical fields oscillating at angular frequencies ω and 2ω to inject and control currents in semiconductors. By changing the relative delay and thus, the relative phase between these two laser fields, the direction and amplitude of the injected photocurrent can be controlled [23–32]. More recently, such a phase-control of photocurrent is also achieved with a single ultrashort laser pulse with a controlled carrier-envelope phase (CEP). In this case, the CEP of the laser pulse takes the role of the relative phase and, thus, controls the injected photocurrent [5, 8, 11, 33-41].

Most of the early experiments have been performed in the resonant regime, where electrons are excited from the valence to the conduction band via the absorption of one or multiple photons. Here, the transient light-induced momentum transfer to electrons is usually neglected [42]. In contrast, when long optical wavelengths or strong electric fields are applied, the light field can significantly change the transient momentum of the electrons and can no longer be neglected [5, 42-45]. This momentum change drives coupled inter- and intra-band electron dynamics, which may span multiple bands and motion throughout the Brillouin zone [3, 46, 47]. The underlying electron dynamics give rise to novel phenomena, which have been pioneered by Mark Stockman and his group [9, 48-53]. Stockman's ground-breaking theoretical predictions were particularly focused, but not limited to the two-dimensional (2D) material graphene, as it serves as an ideal model system to study light-matter interaction. Recently, it has been confirmed that a simple tight-binding model Hamiltonian is sufficient to capture the essential light-field driven electron dynamics in graphene [54].

We have demonstrated the current generation in graphene using a single laser pulse with a controlled CEP [5, 55-57]. In these experiments, we applied the formalism worked out by Mark Stockman and his group [50] and demonstrated how combined inter- and intraband electron dynamics may result in a measurable net current after the exciting laser pulse is gone. The measured current amplitude for the maximal applied field strength of 3.0 V/nm is typically in the range of tens of tens of picoamperes. Recently, we also realized a two-color $\omega + 2\omega$ excitation scheme. By admixing the second harmonic pulse we observed a maximal current of 7 nA, more than two orders of magnitude larger compared to the single-pulse CEP-dependent current [58]. We note that the same laser system and an identical graphene sample were used for both experiments.

In this letter we take these observations as an opportunity to compare both approaches - CEP control and two-color control - and, find and discuss the superior nature of the two-color excitation scheme.

We start our discussion with general requirements for the generation of a residual current in bulk graphene, without applying a bias voltage. To obtain a residual current, an imbalance of excited electrons with respect to the underlying band structure, i.e., net electron momentum, must remain in the system after the pulse is gone. This can be achieved by

Applying a laser pulse that breaks population symmetry in momentum space [5, 54, 57]. Using the Bloch acceleration theorem, $\dot{k}(t) = -\hbar^{-1}eE(t)$, with E(t) the electric field waveform and e the electron charge, the temporal evolution of an electron wavenumber k(t)can be described.

From

$$k(t) = \frac{e}{\hbar} \int_{-\infty}^{t} E(t') dt' = k_0 - \frac{e}{\hbar} A(t), \qquad (1)$$

where k_0 is the initial electron wavenumber, it can be seen that the vector potential A(t) is the quantity responsible for breaking the population symmetry to inject net momentum.

- Interference of electron wave packets via interband dynamics. Without interference, k(t) may be asymmetric, however, as $k(t = -\infty) = k(t = \infty) = k_0$ every electron regains its initial momentum after the laser pulse. Thus, the role of interference is to translate transient momentum asymmetry to a residual population imbalance. In the weak-field limit (i.e., $E_0 \ll 1 \text{ V/nm}$) interference of an odd and an even multiphoton absorption pathway (e.g. $\omega + 2\omega$ interference) [5, 55] or for strong optical fields (i.e., E_0 >> 1 V/nm) interference of electron wavepackets that undergo subsequent Landau-Zener processes may act as the required processes [5, 42, 59].
- To satisfy condition (2), electronic coherence must be maintained sufficiently long.

Since conditions (2) and (3) are of equal importance for current control via the CEP and $\omega + 2\omega$ fields, we focus on the temporal symmetry of the applied laser fields, i.e., condition (1), which can largely differ for the two cases.

In the excitation with a single few-cycle CEP-controlled laser pulse, maximum imbalance of residual conduction band population and therefore the maximum residual current is obtained for a vector potential with different amplitudes for positive and negative half-cycles, as outlined in the above paragraph. Figure 1a with the electric field waveform and Figure 1b for the corresponding vector potential demonstrate that this is given for a CEP of Φ_{CEP} = $\pm \pi/2$. In this case, an electron starting from positive or negative wavenumber accumulates a different dynamical phase between subsequent Landau-Zener transtions, which results in a different interference condition and thus a population imbalance and a residual current.

In case of the two-color $\omega + 2\omega$ excitation scheme, two laser pulses are temporally overlapped, with one pulse oscillating at the fundamental angular frequency ω and the second pulse, which is the second harmonic of the fundamental pulse oscillating at 2ω . In this scheme, the symmetry of A(t) is determined by the relative phase Φ_{rel} between two pulses. When both colors are delayed by $\Phi_{\rm rel}$ $=\pm\pi/2$, as shown in Figure 1c and d, A(t) is again asymmetric with respect to positive and negative amplitudes and thus, net momentum can be transferred to the system.

To quantify the asymmetry and finally compare CEP- and two-color-control, we introduce the asymmetry parameter [60]

$$\Gamma = \left| \frac{A_+}{A_-} \right|,\tag{2}$$

with $A_{+}(t)$ the absolute value of the global maximum and minimum of the resulting vector potential. When $\Gamma = 1$,

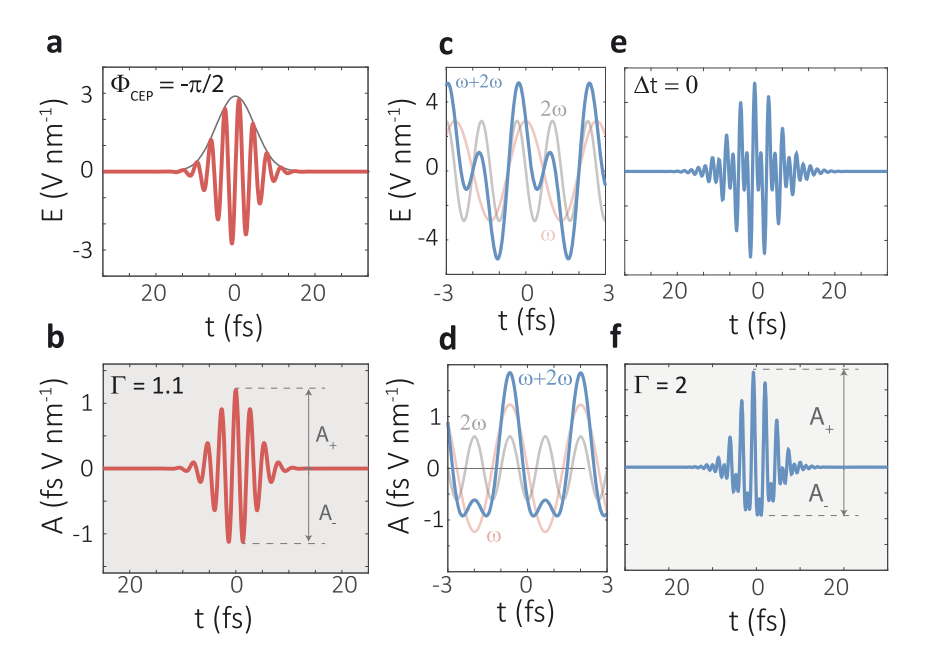


Figure 1: Electric field and vector potential waveform of a single and a two-color laser field. The top panels show the electric field waveform (a, c, and e), with the corresponding vector potential in (b, d, and f). (a) Gaussian electric field waveform for a 5.4 fs laser pulse oscillating at $\omega = 2\pi \cdot 375$ THz and an electric field amplitude of 3 V/nm. The carrier-envelope phase is set to $\Phi_{\text{CEP}} = -\pi/2$. (b) Corresponding vector potential. For $\Phi_{\text{CEP}} = -\pi/2$ the vector potential exhibits a clear peak toward positive values, i.e., $|A_+| > |A_-|$. The asymmetry parameter Γ (see Eq. (2)) is 1.1. (c) Two-color electric field, shown in case of a continuous wave (red: ω and blue: 2ω), with the corresponding vector potential in (d). When both pulses are phase-shifted by $\pi/2$ and the electric field strengths of the ω - and 2ω -pulse are equal (corresponding to a 2:1 ratio in A(t)), the vector potential has its maximal asymmetry with respect to A_+ and A_- ($\Gamma=2$). (e) The two-color electric field with the same field strengths and pulse duration as for the ω -pulse shown in (a) and a $\Phi_{\text{CEP}}=0$, while the 2ω pulse has a pulse duration of 8 fs, a field strength of 3 V/nm and $\Phi_{\text{CEP}}=\pi/2$. These parameters are chosen to visualize the strongly asymmetric vector potential, i.e., $\Gamma=2$ shown in (f).

the maximum value of the vector potential equals its minimum value (up to the sign) and, therefore, A(t) does not break the inversion symmetry. In contrast, for $\Gamma>1$ the vector potential breaks the inversion symmetry and can introduce net momentum [61, 62]. In Figure 1, we show the Γ parameter for both excitation schemes. For the CEP control, we achieve a $\Gamma=1.1$, which is smaller than the one achieved for the $\omega+2\omega$ control ($\Gamma=2$). The larger Γ tells us already that the largest residual current can be expected with the two-color field.

Importantly, for both schemes, a single phase controls the amplitude and the direction of current injected into the graphene. While for CEP control Φ_{CEP} itself is used, the relative phase Φ_{rel} takes over the dominating role for two-color control. Both phases can be straightforwardly accessed experimentally.

We note that the two-color excitation scheme is not limited to $\omega + 2\omega$ pulses. In general $n\omega + m\omega$ excitation, with n and m integer numbers, can result in a residual current if n and m are of different parity [63, 64]. For example, $\omega + 3\omega$ will result in an inversion symmetric vector potential and thus, no current will be generated. In contrast,

higher orders such as n=1 and m=4 or n=2 and m=3 are able to inject a residual current. From an experimental point of view, we focus here on the lowest odd-order process, i.e., $\omega + 2\omega$, since these pulses are easy to generate and typically yield a larger symmetry breaking effect.

In Figure 2 we show experimental data on the realization of CEP control (Figure 2a) and $\omega + 2\omega$ control (Figure 2b) of laser-induced currents in monolayer graphene. The current is measured on a $10 \times 2 \, \mu m^2$ monolayer graphene strip contacted to two gold electrodes. The monolayer graphene is epitaxially grown on 4H-silicon carbide.

In Figure 2a the current is shown, injected by CEP-controlled 5.4 fs near-infrared laser pulses (800 nm central wavelength). The laser pulses are focused tightly to the center of the graphene strip (1.8 μ m $1/e^2$ intensity radius) to reach apeak electric field strength of 2.8 V/nm on the substrate surface. Here, the CEP-dependent current is isolated in a lock-in measurement referenced to the carrier-envelope-offset frequency of the laser pulse train, set to an arbitrary frequency of 3.3 kHz. By moving a fused silica (SiO₂) wedge in the beam path, the CEP is slowly

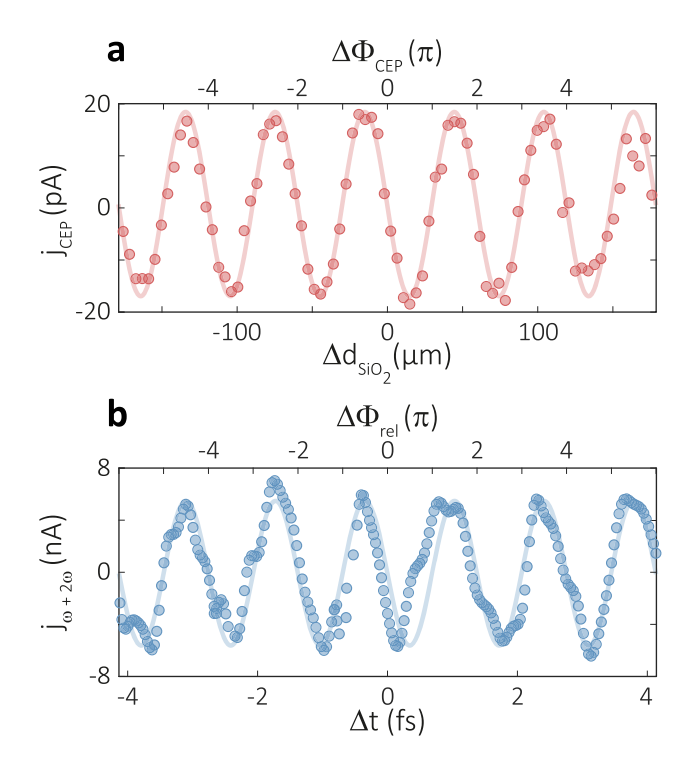


Figure 2: Measured residual current in graphene. (a) CEP-dependent current induced by a single laser pulse as a function of the relative thickness of fused silica in the beam path. A 5.4 fs short pulse at 800 nm central wavelength with 2.8 V/nm peak field strength is applied. (b) Delay-dependent current induced by a $\omega + 2\omega$ laser field as a function of the relative delay. The fundamental pulse has identical properties as in (a), the second harmonic pulse (2ω) at 400 nm central wavelength is 19 fs long and reaches a peak field of 0.3 V/nm. For both experiments (a and b) the laser pulses were focused on identical graphene strips with 10 μ m length such that neighboring electrodes were not illuminated. Clearly, the current is much larger in (b).

modulated on top to control the amplitude and direction of the CEP-dependent current. Clearly, the period of the current signal is directly given by the change of SiO_2 thickness that relates to a change in CEP by $\Delta\Phi=2\pi$, i.e., introducing $\Delta d=\left(\frac{\partial n}{\partial \lambda}|_{\lambda_0=800~\mathrm{nm}}\right)^{-1}=57.5~\mathrm{\mu m}~\mathrm{SiO}_2$ shifts the CEP by 2π . For CEPs of $\pm\pi/2$, the current reaches its maximum amplitude of $\pm18~\mathrm{pA}$, while no current is generated for $\Phi_{\mathrm{CEP}}=0~\mathrm{or}~\pi$.

In a second experiment performed with the identical laser system, we focus two laser pulses with central wavelengths at 800 nm (5.4 fs, 2.8 V/nm) and at 400 nm (19 fs, 0.3 V/nm) to a graphene strip with the same dimensions. This corresponds to a $\omega + 2\omega$ experiment at angular frequencies $\omega = 2\pi \cdot 375$ THz and $2\omega = 2\pi \cdot 750$ THz. Here, the relative phase-dependent current is obtained by changing the delay between both laser pulses with a small oscillatory modulation (719 Hz) on top as a reference for the

lock-in measurement scheme. As shown in Figure 2b, the measured current follows the relative phase between both pulses while its periodicity is given by the 2ω -component. The current induced by the $\omega + 2\omega$ field exceeds the CEP-controlled current by more than two orders of magnitude as it reaches a maximum value at 7 nA. Further details on this measurement can be found in [58].

While the Γ parameter gives a simple estimate on the occurrence and the magnitude of a current, the current generation process is in fact more complex, in particular, if strong and short laser pulses are applied. To compare the magnitude of current injection via $\omega + 2\omega$ electron control with that of an individual CEP-controlled fewcycle laser pulse, we model the dynamics of the light-field driven electrons in graphene using a nearest-neighbor tight-binding model with minimal coupling to the laser field [5, 50, 65]. The residual conduction band population is obtained numerically by integrating the time-dependent Schrödinger equation (TDSE). The injected current is then derived from the residual conduction band population [5, 57]. Given the sub-cycle current generation process on a time scale of less than 2.7 fs, which is shorter than the electron thermalization time constant in graphene [66-68], the electron dynamics can be treated as fully coherent within the TDSE simulation. Subsequent charge propagation toward the electrodes will reduce the measured current amplitude compared to the injected microscopic current. We expect a similar reduction for the $\omega + 2\omega$ and CEP excitation scheme [56] and thus, we can directly compare the residual current densities obtained from the simulations.

First, we apply a single laser pulse with $\Phi_{\rm CEP}=\pi/2$ for various pulse durations from 2 fs to 10 fs and a fixed peak electric field strength of $E_{0,\omega}=2.8$ V/nm. The calculated current is shown in Figure 3a as a red line. When the pulse duration is long ($\tau_{\omega}=8$ fs, Figure 3e) almost no residual current is injected ($\Gamma\approx1$, Figure 3b). Decreasing the pulse duration to 5 fs (Figure 3d, $\Gamma=1.1$) and 3 fs (Figure 3c, $\Gamma=1.3$) increases Γ and a nonzero residual current is observed. We note that the oscillatory nature of the current as a function of the pulse duration can be explained based on the number of optical cycles involved in Landau–Zener–Stückelberg interference of electron wavepackets [5, 42, 59].

The blue line in Figure 3a shows the current originating from the two-color laser field. The pulse duration of the 2ω -pulse is kept at 19 fs, while that of the ω pulse is varied. The peak electric field strengths and the 2ω -pulse duration match the experimental parameters discussed in Figure 2: $E_{\omega} = 2.8 \text{ V/nm}$. $E_{2\omega} = 0.3 \text{ V/nm}$, $\tau_{\omega} = 5.4 \text{ fs}$ and $\tau_{2\omega} = 19 \text{ fs}$.

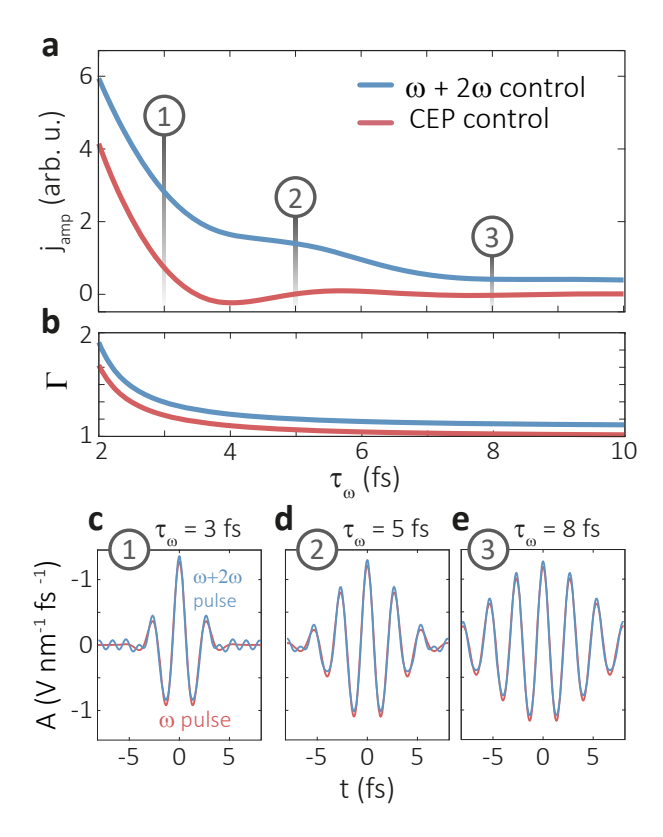


Figure 3: Residual current as a function of pulse duration obtained from TDSE simulations. (a) Residual current induced by a Gaussian laser pulse centered at $\omega=2\pi\cdot375$ THz, $E_{0,\omega}=2.8$ V/nm, $\Phi_{\rm CEP}=\pi/2$ (red line). For $\omega+2\omega$ control (blue line) a Gaussian pulse centered at $2\omega=2\pi\cdot750$ THz with the same CEP and $E_{0,2\omega}=0.3$ V/nm is admixed. In both cases, the pulse duration τ_{ω} of the fundamental (ω) is swept from 2 fs to 10 fs. (b) Corresponding Γ parameter for both schemes. (c–e) Vector potential of the ω -pulse and the $\omega+2\omega$ pulse for $\tau_{\omega}=3,5,8$ fs, see marks in (a).

Here, even for long ω -pulses ($\tau_{\omega} >$ 10 fs), the 2ω contribution significantly breaks the inversion symmetry resulting in $\Gamma = 1.14$ at $\tau_{\omega} =$ 10 fs (Figure 3b). Independent of the fundamental pulse length, the asymmetry introduced by the $\omega + 2\omega$ field always dominates that of the single pulse. Thus, for $\tau_{\omega} = 5.4$ fs, as used in the experiments, the two-color-controlled currents exceed the CEP-controlled ones, both in experiment and TDSE-simulations.

With our theoretical considerations and experimental observations, we demonstrated the generation of residual currents in graphene via control of the CEP of a single fewcycle laser pulse and via control of the relative phase of a $\omega + 2\omega$ field synthesized by two separate laser pulses. We found that the latter field is superior in the current amplitude by two orders of magnitude (18 pA for CEP control vs. 7 nA for two-color-control), which can be explained straightforwardly by the symmetry of its underlying vector potential given by the Γ parameter. Our TDSE simulations

support the superior nature of the two-color excitation scheme compared to the single pulse experiment for the set of given pulse durations of the fundamental laser field ω and its second harmonic 2ω . Despite the larger experimental effort of generating the here applied twocolor laser field, it is of central importance for the ultrafast control of light-field driven phenomena in solids, nanostructures, and gases beyond current generation [62, 69-72]. As it offers highly efficient symmetry breaking and additional degrees of freedom, such as admixture, polarization, and the CEP of both pulses, we expect this scheme to be crucial for the understanding of ultrafast phenomena from the fundamental perspective and for technological relevance. Especially when using tailored light fields with orthogonal polarization, the temporal confinement of charge injection, photoemission, or high-harmonic generation can be largely enhanced by the gating of a 2ω component already at moderate field strengths. Emerging fields such as petahertz electronics may benefit significantly from the increase in signal amplitude and precision that come with it. Or as Mark Stockman put it in one of his last public talks on strongfield physics in 2D-materials [73]: "There is a lot of work, and for experimentalists, if I were you, I would have done it."

Author contribution: All the authors have accepted responsibility for the entire content of this submitted manuscript and approved submission.

Research funding: This work has been supported in part by the Deutsche Forschungsgemeinschaft (SFB 953 "Synthetic Carbon Allotropes"), the PETACom project financed by Future and Emerging Technologies Open H2020 program and ERC grants NearFieldAtto and AccelOnChip. C. H. acknowledges support from the Alexander von Humboldt Foundation and the Max Planck School for Photonics. T. E. appreciates the support of the Friedrich Naumann Foundation for Freedom and the International Max Planck Research School Physics of Light.

Conflict of interest statement: The authors declare no conflicts of interest regarding this article.

References

- [1] F. Krausz and M. I. Stockman, "Attosecond metrology: from electron capture to future signal processing," *Nat. Photonics*, vol. 8, pp. 205–213, 2014.
- [2] A. Schiffrin, T. Paasch-Colberg, N. Karpowicz, et al., "Optical-field-induced current in dielectrics," *Nature*, vol. 493, pp. 70-74, 2013.

- [3] O. Schubert, M. Hohenleutner, F. Langer, et al., "Sub-cycle control of terahertz high-harmonic generation by dynamical Bloch oscillations," Nat. Photonics, vol. 8, pp. 119-123, 2014.
- [4] J. B. Khurgin, "Optically induced currents in dielectrics and semiconductors as a nonlinear optical effect," J. Opt. Soc. Am. B, vol. 33, p. C1, 2016.
- [5] T. Higuchi, C. Heide, K. Ullmann, H. B. Weber, and P. Hommelhoff, "Light-field-driven currents in graphene," Nature, vol. 550, pp. 224-228, 2017.
- [6] J. Reimann, S. Schlauderer, C. P. Schmid, et al., "Subcycle observation of lightwave-driven Dirac currents in a topological surface band," Nature, vol. 562, pp. 396-400, 2018.
- [7] C. Heide, M. Hauck, T. Higuchi, et al., "Attosecond-fast internal photoemission," Nat. Photonics, vol. 14, pp. 219-222, 2020.
- [8] V. Hanus, V. Csajbók, Z. Pápa, et al., "Light-field-driven current control in solids with pJ-level laser pulses at 80 MHz repetition rate," Optica, vol. 8, p. 570, 2021.
- [9] H. K. Kelardeh, V. Apalkov, and M. I. Stockman, "Attosecond strong-field interferometry in graphene: chirality, singularity, and Berry phase," Phys. Rev. B, vol. 93, p. 155434, 2016.
- [10] T. T. Luu, Z. Yin, A. Jain, et al., "Extreme ultraviolet high-harmonic generation in liquids," Nat. Commun., vol. 9, p. 3723, 2018.
- [11] C. Heide, T. Higuchi, H. B. Weber, and P. Hommelhoff, "Coherent electron trajectory control in graphene," Phys. Rev. Lett., vol. 121, p. 207401, 2018.
- [12] R. E. F. Silva, Á. Jiménez-Galán, B. Amorim, O. Smirnova, and M. Ivanov, "Topological strong-field physics on sub-laser-cycle timescale," Nat. Photonics, vol. 13, pp. 849-854, 2019.
- [13] F. Langer, S. Schlauderer, M. Gmitra, et al., "Lightwave valleytronics in a monolayer of tungsten diselenide," Nature, vol. 557, pp. 76-80, 2018.
- [14] S. A. Sato, J. W. McIver, M. Nuske, et al., "Microscopic theory for the light-induced anomalous Hall effect in graphene," Phys. Rev. B, vol. 99, p. 214302, 2019.
- [15] F. Nematollahi, S. Azar Oliaei Motlagh, V. Apalkov, and M. I. Stockman, "Weyl semimetals in ultrafast laser fields," Phys. Rev. B, vol. 99, pp. 1-9, 2019.
- [16] Y. Bai, L. Zhou, J. Wang, et al., "Excitons in strain-induced one-dimensional moiré potentials at transition metal dichalcogenide heterojunctions," Nat. Mater., vol. 19, pp. 1068-1073, 2020.
- [17] D. Baykusheva, A. Chacón, D. Kim, D. E. Kim, D. A. Reis, and S. Ghimire, "Strong-field physics in three-dimensional topological insulators," Phys. Rev., vol. 103, p. 023101, 2021.
- [18] Á. Jiménez-Galán, R. E. F. Silva, O. Smirnova, and M. Ivanov, "Sub-cycle valleytronics: control of valley polarization using few-cycle linearly polarized pulses," Optica, vol. 8, pp. 277-280, 2021.
- [19] M. S. Mrudul, Á. Jiménez-Galán, M. Ivanov, and G. Dixit, "Light-induced valleytronics in pristine graphene," Optica, vol. 8, pp. 422-427, 2020.
- [20] C. P. Schmid, L. Weigl, P. Grössing, et al., "Tunable non-integer high-harmonic generation in a topological insulator," Nature, vol. 593, pp. 385-390, 2021.
- [21] F. Siegrist, J. A. Gessner, M. Ossiander, et al., "Light-wave dynamic control of magnetism," Nature, vol. 571, pp. 240-244, 2019.

- [22] K. Jonas, P. Zimmermann, A. W. Holleitner, and C. Kastl, "Light-field and spin-orbit-driven currents in van der Waals materials," Nanophotonics, vol. 9, pp. 2693-2708, 2020.
- [23] G. Kurizki, M. Shapiro, and B. Paul, "Phase-coherent control of photocurrent directionality in semiconductors," Phys. Rev. B, vol. 39, pp. 3435-3437, 1989.
- [24] E. Dupont, P. B. Corkum, H. C. Liu, M. Buchanan, and Z. R. Wasilewski, "Phase-controlled currents in semiconductors," Phys. Rev. Lett., vol. 74, pp. 3596-3599, 1995.
- [25] R. Atanasov, A. Haché, J. L. P. Hughes, H. M. Van Driel, and J. E. Sipe, "Coherent control of photocurrent generation in bulk semiconductors," Phys. Rev. Lett., vol. 76, pp. 1703-1706,
- [26] A. Haché, Y. Kostoulas, R. Atanasov, J. L. P. Hughes, J. E. Sipe, and H. M. van Driel, "Observation of coherently controlled photocurrent in unbiased, bulk GaAs," Phys. Rev. Lett., vol. 78, pp. 306-309, 1997.
- [27] N. Laman, A. I. Shkrebtii, J. E. Sipe, and H. M. Van Driel, "Quantum interference control of currents in CdSe with a single optical beam," Appl. Phys. Lett., vol. 75, pp. 2581-2583, 1999.
- [28] J. L. Hall, S. T. Cundiff, D. J. Jones, et al., "Carrier-envelope phase control of femtosecond mode-locked lasers and direct optical frequency synthesis carrier-envelope phase control of femtosecond mode-locked lasers and direct optical frequency synthesis," Science, vol. 288, pp. 635-639, 2000.
- D. Sun, C. Divin, J. Rioux, et al., "Coherent control of ballistic photocurrents in multilayer epitaxial graphene using quantum interference," Nano Lett., vol. 10, pp. 1293-1296, 2010.
- [30] J. Rioux, B. Guido, and J. E. Sipe, "Current injection by coherent one- and two-photon excitation in graphene and its bilayer," Phys. Rev. B, vol. 83, pp. 1-9, 2011.
- [31] H. Tahara and Y. Kanemitsu, "Dynamical coherent control of photocurrent in bulk GaAs at room temperature," Phys. Rev. B, vol. 90, p. 245203, 2014.
- [32] R. A. Muniz, C. Salazar, K. Wang, S. T. Cundiff, and J. E. Sipe, "Quantum interference control of carriers and currents in zinc blende semiconductors based on nonlinear absorption processes," Phys. Rev. B, vol. 100, p. 075202, 2019.
- [33] T. M. Fortier, P. A. Roos, D. J. Jones, S. T. Cundiff, R. D. R Bhat, and J. E. Sipe, "Carrier-envelope phase-controlled quantum interference of injected photocurrents in semiconductors," Phys. Rev. Lett., vol. 92, p. 147403, 2004.
- [34] P. A. Roos, X. Li, J. A. Pipis, et al., "Characterization of carrier-envelope phase-sensitive photocurrent injection in a semiconductor," J. Opt. Soc. Am. B, vol. 22, p. 362, 2005.
- [35] T. Paasch-Colberg, A. Schiffrin, N. Karpowicz, et al., "Solid-state light-phase detector," Nat. Photonics, vol. 8, pp. 214-218, 2014.
- [36] T. Rybka, M. Ludwig, M. F. Schmalz, V. Knittel, D. Brida, and A. Leitenstorfer, "Sub-cycle optical phase control of nanotunnelling in the single-electron regime," Nat. Photonics, vol. 10, pp. 667-670, 2016.
- [37] M. Ludwig, G. Aguirregabiria, F. Ritzkowsky, et al., "Sub-femtosecond electron transport in a nanoscale gap," Nat. Phys., vol. 16, pp. 341-345, 2019.
- [38] F. Langer, Y.-P. Liu, Z. Ren, et al., "Few-cycle lightwave-driven currents in a semiconductor at high repetition rate," Optica, vol. 7, p. 276, 2020.

- [39] Y. Yang, M. Turchetti, P. Vasireddy, et al., "Light phase detection with on-chip petahertz electronic networks," Nat. Commun., vol. 11, p. 3407, 2020.
- [40] G. M. Rossi, R. E. Mainz, Y. Yang, et al., "Sub-cycle millijoule-level parametric waveform synthesizer for attosecond science," Nat. Photonics, vol. 14, pp. 629-635, 2020.
- [41] M. R. Bionta, F. Ritzkowsky, M. Turchetti, et al., "On-chip sampling of optical fields with attosecond resolution," Nat. Photonics, vol. 15, pp. 456-460, 2021.
- [42] C. Heide, T. Boolakee, T. Higuchi, and P. Hommelhoff, Adiabaticity Parameters for the Categorization of Light-Matter Interaction – from Weak to Strong Driving, arXiv:2104.10112,
- [43] L. V. Keldysh, "Ionization in the field of a strong electromagnetic wave," Sov. Phys. JETP, vol. 20, pp. 1307-1314, 1965.
- [44] M. S. Wismer, S. Yu Kruchinin, M. Ciappina, M. I. Stockman, and V. S. Yakovlev, "Strong-field resonant dynamics in semiconductors," Phys. Rev. Lett., vol. 116, p. 197401, 2016.
- [45] S. Y. Kruchinin, F. Krausz, and V. S. Yakovlev, "Colloquium: strong-field phenomena in periodic systems," Rev. Mod. Phys., vol. 90, p. 21002, 2018.
- [46] S. Ghimire, A. D. Dichiara, E. Sistrunk, P. Agostini, L. F. Dimauro, and D. A. Reis, "Observation of high-order harmonic generation in a bulk crystal," Nat. Phys., vol. 7, pp. 138-141,
- [47] N. Yoshikawa, T. Tamaya, and K. Tanaka, "Optics: highharmonic generation in graphene enhanced by elliptically polarized light excitation," Science, vol. 356, pp. 736-738,
- [48] H. K. Kelardeh, V. Apalkov, and M. I. Stockman, "Wannier-Stark states of graphene in strong electric field," Phys. Rev. B, vol. 90, p. 085313, 2014.
- [49] T. Higuchi, M. I. Stockman, and P. Hommelhoff, "Strong-field perspective on high-harmonic radiation from bulk solids," Phys. Rev. Lett., vol. 113, p. 213901, 2014.
- [50] H. K. Kelardeh, V. Apalkov, and M. I. Stockman, "Graphene in ultrafast and superstrong laser fields," Phys. Rev. B, vol. 91, p. 045439, 2015.
- [51] S. Azar Oliaei Motlagh, F. Nematollahi, V. Apalkov, and M. I. Stockman, "Topological resonance and single-optical-cycle valley polarization in gapped graphene," Phys. Rev. B, vol. 100, p. 115431, 2019.
- [52] S. Azar Oliaei Motlagh, V. Apalkov, and M. Stockman, "Laser pulse waveform control of Dirac fermions in graphene," in Proceedings of SPIE - The International Society for Optical Engineering, vol. 44, 2019.
- [53] S. Azar Oliaei Motlagh, V. Apalkov, and M. I. Stockman, "Transition metal dichalcogenide monolayers in an ultrashort optical pulse: femtosecond currents and anisotropic electron dynamics," Phys. Rev. B, vol. 103, p. 155416, 2021.
- [54] Q. Z. Li, P. Elliott, J. K. Dewhurst, S. Sharma, and S. Shallcross, "Ab initio study of ultrafast charge dynamics in graphene," Phys. Rev. B, vol. 103, p. L081102, 2021.
- [55] C. Heide, T. Boolakee, T. Higuchi, H. B. Weber, and P. Hommelhoff, "Interaction of carrier envelope phase-stable laser pulses with graphene: the transition from the weak-field to the strong-field regime," New J. Phys., vol. 21, p. 045003, 2019.

- [56] T. Boolakee, C. Heide, F. Wagner, et al., "Length-dependence of light-induced currents in graphene," J. Phys. B: At., Mol. Opt. Phys., vol. 53, p. 154001, 2020.
- [57] C. Heide, T. Boolakee, T. Higuchi, and P. Hommelhoff, "Sub-cycle temporal evolution of light-induced electron dynamics in hexagonal 2d materials," JPhys Photonics, vol. 2, p. 024004, 2020.
- [58] C. Heide, T. Eckstein, T. Boolakee, et al., Electronic Coherence and Coherent Dephasing in the Optical Control of Electrons in Graphene, 2021, http://arxiv.org/abs/2107.06848.
- [59] S. N. Shevchenko, S. Ashhab, and F. Nori, "Landau-Zener-Stückelberg interferometry," Phys. Rep., vol. 492, pp. 1-30, 2010.
- [60] A. J. Garzón-Ramírez and I. Franco, "Symmetry breaking in the Stark control of electrons at interfaces (SCELI)," J. Chem. Phys., vol. 153, p. 044704, 2020.
- [61] A. J. Garzón-Ramírez and I. Franco, "Stark control of electrons across interfaces," Phys. Rev. B, vol. 98, p. 121305(R), 2018.
- [62] F. Navarrete and U. Thumm, "Two-color-driven enhanced high-order harmonic generation in solids," Phys. Rev. A, vol. 102, p. 063123, 2020.
- [63] I. Franco and P. Brumer, "Minimum requirements for laser-induced symmetry breaking in quantum and classical mechanics," J. Phys. B Atom. Mol. Opt. Phys., vol. 41, p. 074003, 2008.
- [64] M. Shapiro and P. Brumer, Quantum Control of Molecular Processes, Weinheim, John Wiley & Sons, 2012.
- [65] K. L. Ishikawa, "Nonlinear optical response of graphene in time domain," Phys. Rev. B, vol. 82, p. 201402(R), 2010.
- [66] I. Gierz, J. C. Petersen, M. Mitrano, et al., "Snapshots of non-equilibrium Dirac carrier distributions in graphene," Nat. Mater., vol. 12, pp. 1119-1124, 2013.
- [67] M. Breusing, S. Kuehn, T. Winzer, et al., "Ultrafast nonequilibrium carrier dynamics in a single graphene layer," Phys. Rev. B, vol. 83, p. 153410, 2011.
- [68] K. J. Tielrooij, L. Piatkowski, M. Massicotte, et al., "Generation of photovoltage in graphene on a femtosecond timescale through efficient carrier heating," Nat. Nanotechnol., vol. 10, pp. 437-443, 2015.
- [69] H. Niikura, N. Dudovich, D. M. Villeneuve, and P. B. Corkum, "Mapping molecular orbital symmetry on high-order harmonic generation spectrum using two-color laser fields," Phys. Rev. Lett., vol. 105, p. 053003, 2010.
- [70] G. Vampa, T. J. Hammond, N. Thiré, et al., "Linking high harmonics from gases and solids," Nature, vol. 522, pp. 462-464, 2015.
- [71] M. Förster, T. Paschen, M. Krüger, et al., "Two-color coherent control of femtosecond above-threshold photoemission from a Tungsten nanotip," Phys. Rev. Lett., vol. 117, pp. 1-6, 2016.
- [72] S. Sederberg, F. Kong, F. Hufnagel, C. Zhang, E. Karimi, and P. B. Corkum, "Vectorized optoelectronic control and metrology in a semiconductor," Nat. Photonics, vol. 14, pp. 680-685, 2020.
- [73] M. I. Stockman, "Solids in ultrafast strong laser fields: topological nanophotonic phenomena (conference presentation)," in Proc. volume 11080, metamaterials, metadevices, and metasystems 2019, San Diego, CA, USA, 2019, p. 110800C.